Hindawi
International Journal of Chemical Engineering
Volume 2020, Article ID 8818455, 14 pages
https://doi.org/10.1155/2020/8818455

Research Article

Removal of Ammonium from Aqueous Solutions Using Zeolite Synthesized from Electrolytic Manganese Residue

Changxin Li,[1] **Yuan Yu**,[1] **Qingwu Zhang**,[1] **Hong Zhong**,[2] **and Shuai Wang**[2]

[1]*College of Safety Science and Engineering, Nanjing Tech University, Nanjing 211816, Jiangsu, China*
[2]*College of Chemistry and Chemical Engineering, Central South University, Changsha 410083, Hunan, China*

Correspondence should be addressed to Changxin Li; lichangxin2010@njtech.edu.cn

Received 13 June 2020; Revised 18 August 2020; Accepted 3 September 2020; Published 14 September 2020

Academic Editor: Andreas Bück

This paper carried out the study on removal of ammonium from aqueous solutions by zeolite derived from electrolytic manganese residue (EMR) via a fusion method. The variables of pH, contact time, EMRZ (EMR-based zeolite) dosage, initial ammonium concentration, and competitive cations and anions on the ammonium uptake capacity were systematically investigated in an attempt to illustrate adsorption performance of EMRZ. The results show that these influence factors had a remarkable impact on the ammonium uptake capacity of EMRZ. Maximum ammonium uptake capacity was achieved at pH value 8.0, EMRZ dosage 0.2 g/100 mL, contact time 100 min, initial ammonium concentration 200 mg/L, and temperature 35°C. Under optimized conditions, ammonium uptake capacity onto EMRZ was up to 27.89 mg/g. The competitive degree of cations in ammonium adsorption process follows the sequence of $Na^+ > K^+ > Ca^{2+} > Mg^{2+}$, and the sequence of anion effect on ammonium removal onto EMRZ is $CO_3^{2-} > Cl^- > SO_4^{2-} > PO_4^{3-}$. The adsorption kinetic was explored and best represented by pseudo-second-order kinetic model. And the adsorption isotherm experimental data had best fitness with the Freundlich and Koble–Corrigan model, suggesting that heterogeneous uptake was the principal mechanism adopted in the process of ammonium adsorption. Moreover, calculation of thermodynamic parameters such as change in free energy (ΔG), enthalpy (ΔH), and entropy (ΔS) was carried out and it was determined to be −15.77~−14.03 kJ·mol^{-1}, +37.66 kJ·mol^{-1}, and +173.38 J·mol^{-1}·K^{-1}, respectively. These parameters confirmed that ammonium uptake onto EMRZ was an endothermic and spontaneous process. Moreover, no obvious deterioration tendency was observed for the regenerated EMRZ compared with fresh EMRZ. These results indicate that EMRZ has wide application prospects in removing ammonium from wastewater.

1. Introduction

It is known that the accumulation of ammonium causes eutrophication in lakes, ponds, and reservoirs; what is more is that it creates a larger demand of oxygen by aquatic life and exposes them to toxicity at the same time [1–6]. With people's understanding of the detrimental influences of ammonium getting to a more profound level nowadays, authorities have established stringent regulations and laws to restrict ammonium discharges. Thus, treatment on wastewater with high ammonia concentration is required prior to discharge into the receiving water. Hence, efficient removal techniques for ammonia in the wastewater are now required.

Ammonia can be removed from wastewater in various ways, including nitrification and denitrification, ammonia stripping, ion exchange, and breakpoint chlorination. Among the proposed processes, ion exchange with zeolite material has been acknowledged to be efficient and cost-effective on account of its low cost and easy operation [7–9]. Generally, the zeolites with open and solid three-dimensional honeycomb structure have a high CEC (cation exchange capacity) and great affinity for ammonia [10–12]. Therefore, the application of ammonium removal using zeolite has caught lots of eyeballs these days.

As we all know, the domestic production capacity of electrolytic manganese metal (EMM) is over 2.11 Mt/a, which covers around 98% of the global EMM production per year. Electrolytic manganese residue (EMR) is a byproduct during the process of producing electrolytic metal manganese (EMM) [13]. At present, for every ton of EMM

produced, 10~12 tons of EMR will be produced and discharged into the landfill sites. It is foreseen that there is a rise in generation rate of EMR as the grade of manganese ore is decreasing. Nowadays in China, almost all EMR are piled up into nearby landfill sites with no treatment except for a small proportion being used as building material [14, 15]. Under the condition of long-term weathering, the pollutants in EMR will gradually migrate and penetrate into the surrounding soil and water, causing environmental pollution problems. In addition, disposal of tons of EMR will also bring great economic burden to the enterprise due to high maintenance and new storage site costs. Thus, considering environmental protection and sustainable development, new recycling techniques for EMR have to be developed. Lately, our research group discovered that the zeolite material can be prepared from the silicon aluminum component in the EMR, which is an eco-friendly way to utilize EMR. Moreover, utilization of solid wastes generated from various industries to prepare related products was not only economical but also in line with the concept of green development [16–18].

At present, there are plenty of studies concerning removal of ammonium from aqueous solutions with different kinds of zeolites available [19–21]. However, investigation on the performance of EMRZ for ammonium removal has rarely been conducted. Accordingly, this work aims to examine the potential of EMRZ for removing ammonia ions from aqueous solutions under various conditions. Moreover, the adsorption characteristics of ammonium ion including equilibrium isotherms, thermodynamic parameters, and adsorption kinetics by EMRZ were also systematically investigated.

2. Materials and Methods

2.1. Materials. The EMR used in this study was obtained from an EMM plant located in Hunan Province, China. The main chemical composition of EMR was determined and listed hereafter, in mass%: $Na_2O = 2.7$, $SiO_2 = 24.6$, $Al_2O_3 = 12.2$, $MgO = 1.7$, $K_2O = 2.4$, $CaO = 8.6$, $MnO = 4.6$ and $Fe_2O_3 = 7.9$. The EMRZ was prepared using the silicon aluminum component in the EMR via a fusion method. The detailed preparation and characterization process of EMRZ is as described in our previous related studies [22]. From the x-ray diffraction (XRD) data (see Figure 1), zeolite A was identified as a major phase component of the synthesized EMRZ, with a small part of zeolite P. The morphology and particle size of EMRZ observed by field emission scanning electron microscopy (FE-SEM) confirmed that highly ordered cubes of zeolite A as well as a small amount of round crystals (zeolite P) were presented (see Figure 2) in EMRZ. Meanwhile, the CEC (cation exchange capacity) and SSA (specific surface area) were 3.45 meq/g and 39.38 m^2/g, respectively. And the CEC of EMRZ (i.e., 3.45 meq/g) is far higher than the relevant zeolites reported in the literature [9, 20, 21], which implies that the EMRZ can be used as a cation exchange material for ammonium adsorption.

All inorganic chemicals in the study, such as NH_4Cl (purity 99.8%), NaCl (purity 99.5%), KCl (purity 99.8%), $CaCl_2$ (purity 96.0%), $MgCl_2$ (purity 99.0%), Na_2SO_4 (purity 99.0%), Na_2CO_3 (purity 99.8%), and $Na_3PO_4\,12H_2O$ (purity 98.0%), were of analytical grade and supplied by Sinopharm Chemical Reagent Co., Ltd. Ammonium stock solution (500 mg NH_4^+-N/L) was prepared using anhydrous salts of NH_4Cl supplied by freshly double-distilled water.

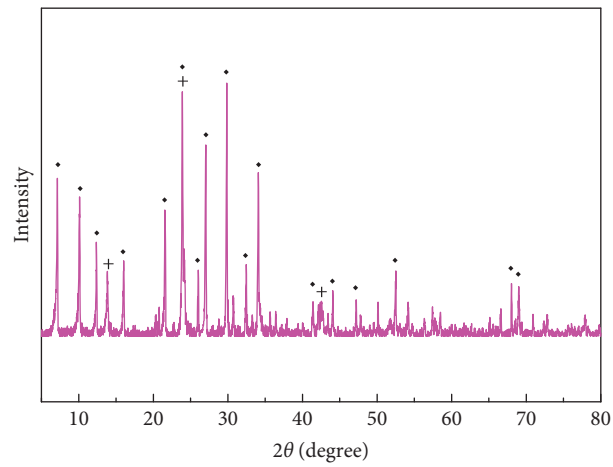

Figure 1: The XRD patterns of EMRZ samples.

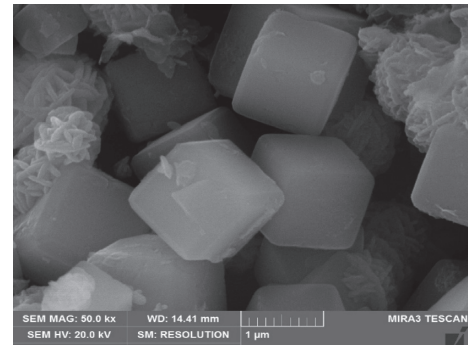

Figure 2: FE-SEM images of EMRZ.

2.2. Adsorption Studies. Batch adsorption analysis was conducted in a thermostatic shaker, which was capable of controlling the temperature at the pre-set value. For each adsorption experiment, 0.2 g of EMRZ was firstly added to a 250 mL conical flask having 100 mL of a predetermined initial ammonium concentration solution at desirable pH value (adjusted using 0.1 mol/L HCl or 0.1 mol/L NaOH solution). Then, the flask was placed in a thermostatic shaker at the controlled temperature and shaken at 200 rpm for a given period. After reaching the predetermined time, the suspension was finally separated by filtration via 0.45 μm filter and the ammonia concentration in the filtrate was analyzed by the method described in characterization section. The ammonium adsorbed on EMRZ was evaluated and calculated according to

$$q_e = \frac{(C_0 - C_e)V}{m}, \quad (1)$$

where C_0 represents the initial ammonium concentration (mg/L) and C_e represents the equilibrium ammonium concentration (mg/L), q_e (mg/g) is ammonium uptake capacity of EMRZ (mg/g), V is the solution volume (L), and m is the mass of EMRZ used (g).

For determining the most favorable process parameters for ammonium removal by EMRZ, batch ammonium adsorption studies have been executed to study the influence of different factors such as contact time, pH, EMRZ dosage, initial ammonium concentration, and competitive cations (K^+, Ca^{2+}, Na^+, and Mg^{2+}) and anions (PO_4^{3-}, SO_4^{2-}, Cl^-, and CO_3^{2-}) on ammonium adsorption capacity.

2.3. EMRZ Regeneration. In this study, the used EMRZ was regenerated by NaCl solution (1 mol/L) treatment, since the "NaCl regeneration" method stood out in all methods [23]. In regeneration process, the used EMRZ was mixed with 1 mol/L NaCl solution at L/S ratio 15 : 1. Then, the mixture was stirred at 200 rpm at 25°C for 12 h and the regeneration was performed two times. Finally, the solid samples were filtered, washed, dried, and sieved through a 100 mesh for further analysis. And comparison was made between the ammonium uptake capacity obtained using regenerated samples and those obtained using fresh EMRZ ones.

2.4. Characterization. X-ray diffractometer (D8 Discover, Bruker, Germany) was used to study the phase composition of different samples. The chemical composition of different samples was determined by XRF (x-ray fluorescence spectrometer) (Axios, PANalytical, Holland). The morphological structure of the synthesized EMRZ was analyzed by field emission scanning electron microscopy (FE-SEM) (Mira3, Tescan, Czech Republic). BET (Brunauer–Emmett–Teller) equation by N_2 adsorption method on ASAP2020 (Micromeritics, USA) was used to determine the SSA. The study of Zhang et al. was used to measure CEC of EMRZ [24]. The ammonium concentration in the resulting solution was determined by the conventional Nesslerization method.

3. Results and Discussion

3.1. Effect of Contact Time. Results of ammonium uptake capacity of EMRZ versus contact time in ammonium solutions are given in Figure 3. As displayed in Figure 3, in the first 100 min, the ammonium uptake capacity of EMRZ was fast; thereafter, the uptake amount of ammonium onto EMRZ became almost stable for all the concentrations studied. This behavior is likely to be induced by the fact that almost all adsorption sites of EMRZ were empty and the concentration gradient of ammonium was high in the beginning. Therefore, the rapid utilization of the most easily available adsorption sites of EMRZ made high-speed diffusion and realization of rapid equilibrium possible. Namely, the quick utilization of the most readily available adsorbing sites of the EMRZ leads to fast diffusion and attainment of rapid equilibrium [25–27]. Based on these results and analysis, the contact time of 100 min was used in the following experiment.

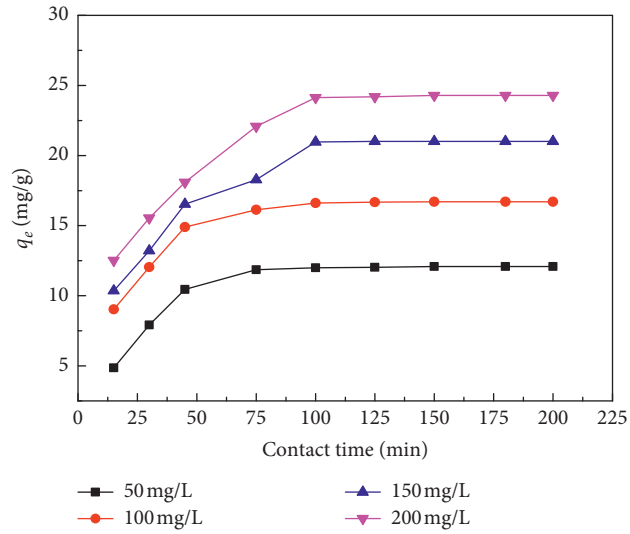

Figure 3: Effect of contact time on ammonium adsorption (EMRZ dosage = 0.2 g/100 mL; pH value = 6.0; temperature = 25°C).

3.2. Effect of pH. To probe into the influence of pH value on ammonium uptake capacity of EMRZ, ammonium removal by EMRZ under diverse pH values ranging from 3.0 to 12.0 was investigated. As shown in Figure 4, the amount of ammonium uptake was raised from 3.24 to 18.2 mg/g, when pH value of solution changed from 3.0 to 8.0. And when the pH was 8.0, ammonium uptake reached the maximum amount. Afterwards, a substantial decrease occurred in the amount of ammonium uptake when pH increased to 12.0. This trend of ammonium uptake is in agreement with the observations stated in literature published earlier [25, 28, 29]. This behavior is caused by the fact that at higher pH (pH > 8.0) part of the ammonium ions are transformed to aqueous ammonia, which cannot be removed by EMRZ via ion exchange. And the lower ammonium uptake obtained at lower pH (pH < 8.0) can be explained by the fact that along with the decrease of pH value the concentration of hydrogen ion rises and the ammonium ions turn into competition mode against hydrogen ions among the exchange sites. Meanwhile, it is also likely that EMRZ starts to break down or dissolve, particularly when the pH is below 4.0 [24].

3.3. Effect of EMRZ Dosage. Figure 5 displays the results of experiments in which the effects of EMRZ dosage on ammonium uptake capacity are determined. As seen in Figure 5, the ammonium uptake capacity reduced from 18.2 to 3.38 mg/g while EMRZ dosage increased from 0.2 to 2.0 g/100 mL. Considering that the initial ammonium concentration stays constant despite changes in EMRZ dosage, it is only natural that the ammonium concentration gradient per unit mass of EMRZ decreases when EMRZ dosage increases. Thus, the driving force for ammonium adsorption generated from high concentration gradient inevitably decreases under this condition. That is to say, when the ammonium exchange with cations in the EMRZ was fully completed at a specific dosage, the ammonium removal reached equilibrium and

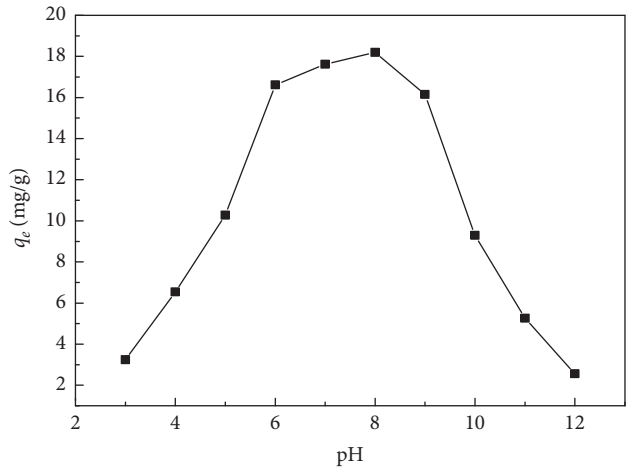

Figure 4: Effect of pH on ammonium adsorption (EMRZ dosage = 0.2 g/100 mL; initial ammonium concentration = 100 mg/L; temperature = 25°C; contact time = 100 min).

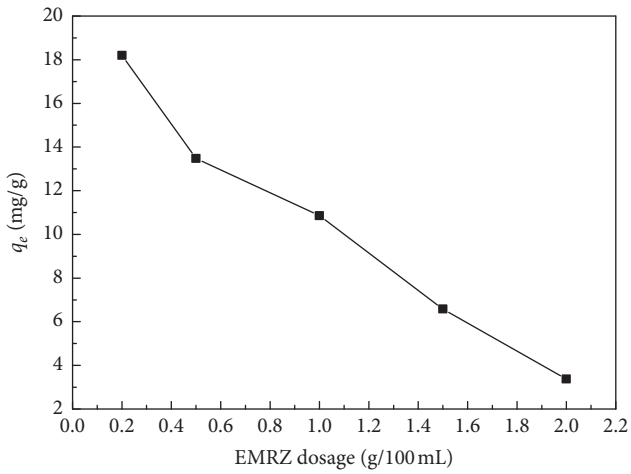

Figure 5: Effect of EMRZ dosage on ammonium adsorption (initial ammonium concentration = 100 mg/L; temperature = 25°C; contact time = 100 min; pH value = 8.0).

much more exchangeable sites of the EMRZ remained unexchanged [24, 30, 31]. On the other hand, the development of aggregates or particle precipitate can been caused under high EMRZ dosage, leading to total surface area of the EMRZ getting reduced and diffusional path length getting increased [32, 33].

3.4. Effect of Initial Ammonium Concentration. For the purpose of analyzing the effect of the initial ammonium concentration, ammonium uptake capacity of EMRZ was investigated at various initial ammonium concentrations. As seen in Figure 6, the adsorption data clearly indicated that the ammonium uptake capacity of EMRZ increases along with the increase in initial ammonium concentration. It can be attributed to the fact that higher initial ammonium concentration supplied a larger mass transfer driving force resulting from concentration gradient [34, 35]. Consequently, the ammonium ions were able to move from outer

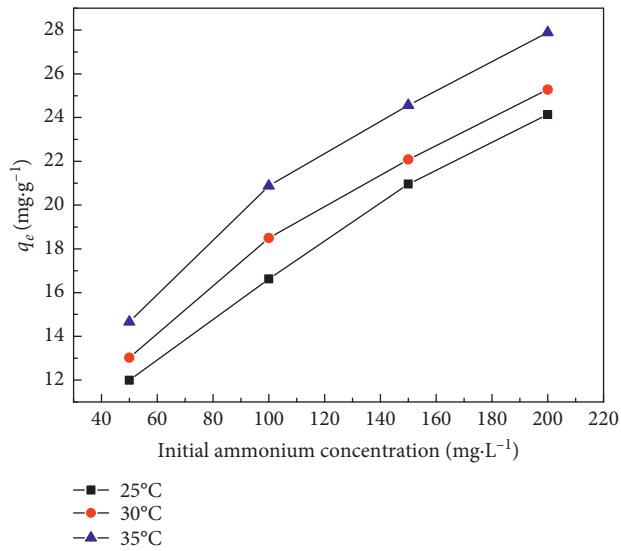

Figure 6: Effect of initial ammonium concentration on ammonium adsorption (EMRZ dosage = 0.2 g/100 mL; contact time = 100 min; pH value = 8.0).

surface to inner micropores of EMRZ to take the place of cations on the surface of EMRZ within certain contact time. Meanwhile, as temperature rises, the ammonium uptake capacity onto EMRZ increases. This may be contributed by the fact that uptake of ammonium onto EMRZ is controlled by an endothermic process. That is to say, the higher temperature is favorable to endothermic reaction once equilibrium is achieved. Therefore, ammonium ions can easily adsorb from the bulk phase by EMRZ with an increase in the temperature of the solution.

3.5. Effect of Competitive Cations. Figure 7 shows the experimental results for ammonium removal by EMRZ in the presence of each competitive cation including K^+, Ca^{2+}, Na^+, and Mg^{2+} ions. As seen in Figure 7, there is a reduction on ammonium adsorption to some extent in the presence of competitive cations in each case. Because K^+, Ca^{2+}, Na^+, and Mg^{2+} ions present in the solution can compete with the ammonium for the available ion-exchange sites on the EMRZ, resulting in a decrease in the uptake amount of ammonium onto EMRZ [36–38], with increasing the concentrations of Mg^{2+}, Ca^{2+}, K^+, and Na^+ from 0 mg/L to 250 mg/L, the uptake amount of ammonium onto EMRZ decreased from 16.62 to 12.98, 11.25, 9.06, and 8.52 mg/g, respectively. At the identical concentration level of competitive cations, the reduction follows the sequence of $Na^+ > K^+ > Ca^{2+} > Mg^{2+}$, indicating the competitive degree of cations in the process of adsorbing ammonium followed the same sequence of $Na^+ > K^+ > Ca^{2+} > Mg^{2+}$. Comparable results can be found in other researches published earlier [21, 39, 40]. However, there are studies that show different results for the competitive degree of zeolite toward those cations. Zhang et al. [24] reported that the competitive degree for cations on the fly ash-made zeolite was $K^+ > Ca^{2+} > Na^+ > Mg^{2+}$. Karadag et al. [41] demonstrated the

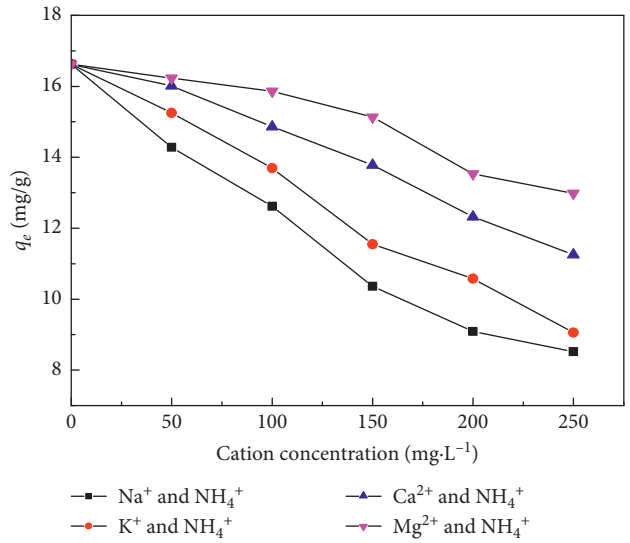

Figure 7: Effect of cations concentration on ammonium adsorption (EMRZ dosage = 0.2 g/100 mL; contact time = 100 min; pH value = 8.0; initial ammonium concentration = 100 mg/L; temperature = 25°C).

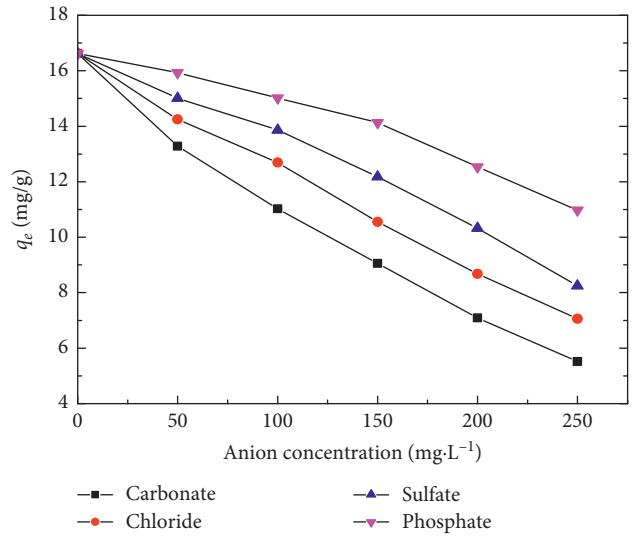

Figure 8: Effect of anions concentration on ammonium adsorption (EMRZ dosage = 0.2 g/100 mL; contact time = 100 min; pH value = 8.0; initial ammonium concentration = 100 mg/L; temperature = 25°C).

competitive degree of four cations on ammonium adsorption by natural clinoptilolite as $K^+ > Na^+ > Ca^{2+} > Mg^{2+}$. The fact that various zeolites possess different characteristics and therefore various competitive degrees for cations can serve as the explanation for these unaligned results.

3.6. Effect of Anions. Figure 8 demonstrates the impact on ammonium removal by EMRZ triggered by anion species as a function of different anions concentrations. It is interesting to notice from Figure 8 that the ammonium uptake is negatively impacted by anions; i.e., the ammonium adsorption capacity went down while anions concentration went up. When the concentration of carbonate, phosphate, sulfate, and chloride ion increased from 50 mg/L to 250 mg/L in the ammonium solution, the ammonium uptake amount fell from 16.62 to 5.52, 10.98, 8.25, and 7.06 mg/g, respectively, which is an indication that the order of anion effect on ammonium adsorption onto EMRZ is $CO_3^{2-} > Cl^- > SO_4^{2-} > PO_4^{3-}$. The explanation mechanism of the phenomenon was plausible as the existence of the anion ions might increase the surface tension of the aqueous phase to the degree of reducing access of ammonium to the micropores and macropores of the EMRZ [24, 42].

3.7. Adsorption Kinetics. The adsorption kinetics of ammonium is extremely important to clarify the adsorption process and the rate-controlling mechanism of ammonium uptake onto EMRZ. In this study, (A) pseudo-first-order kinetic model, (B) pseudo-second-order kinetic model, (C) Elovich equation kinetic model, and (D) intra-particle diffusion kinetic model were employed to test the investigational data [43–46]. And the above adsorption kinetic models can be summarized as follows:

$$\begin{aligned} \ln(q_e - q_t) &= \ln q_e - k_1 t, \\ \frac{t}{q_t} &= \frac{1}{k_2 q_e^2} + \frac{t}{q_e}, \\ q_t &= \left(\frac{1}{\beta}\right)\ln(\alpha\beta) + \left(\frac{1}{\beta}\right)\ln t, \\ q_t &= k_{id} t^{1/2} + C, \end{aligned} \tag{2}$$

where q_e and q_t represent the ammonium adsorption capacity of EMRZ (mg·g^{-1}) at equilibrium and at time t, respectively, k_1 (min^{-1}) and k_2 (g·mg^{-1}·min^{-1}) are the rate constants of pseudo-first-order kinetic and pseudo-second-order kinetic models, respectively, α is the initial adsorption rate (mg·g^{-1}·min^{-1}) and β is associated with the extent of surface coverage and activation energy (g·mg^{-1}), k_{id} is the intra-particle diffusion rate constant (mg·min$^{-1/2}$·g^{-1}), and C stands for the intercept.

Table 1 and Figure 9 demonstrate the linearized kinetic data using the above models, as well as the calculated constants. Comparing the correlation coefficients (R^2) displayed in Figure 9 and Table 1, the correlation coefficients ($R^2 = 0.9925$, 0.9982, 0.9962, and 0.9949) obtained under different initial ammonium concentration (50, 100, 150, and 200 mg/L) for the pseudo-second-order kinetic model were much higher than the ones obtained for the pseudo-first-order kinetic model ($R^2 = 0.7714$, 0.8708, 0.7760, and 0.8102), Elovich equation model ($R^2 = 0.8327$, 0.8420, 0.8496, and 0.9438), and intra-particle diffusion model ($R^2 = 0.6740$, 0.6826, 0.8331, and 0.8719). As shown in Table 1, the calculated q_e is also within close range of the experimental value (q_e (exp)) at 50, 100, 150, and 200 mg/L initial ammonium concentrations. Consequently, it is obvious that the pseudo-second-order kinetic model is of higher accuracy during the

Table 1: Kinetic parameters for ammonia removal using various kinetic models.

Ammonium concentration ($mg \cdot L^{-1}$)	q_e (exp) ($mg \cdot g^{-1}$)	Pseudo-first-order model			Pseudo-second-order model			Elovich equation model			Intra-particle diffusion model	
		q_e ($mg \cdot g^{-1}$)	k_1 (min^{-1})	α ($mg \cdot g^{-1} \cdot min^{-1}$)	q_e ($mg \cdot g^{-1}$)	k_2 ($g \cdot mg^{-1} \cdot min^{-1}$)	R^2	α ($mg \cdot g^{-1} \cdot min^{-1}$)	β ($g \cdot mg^{-1}$)	R^2	k_{id} ($mg \cdot min^{-1/2} \cdot g^{-1}$)	R^2
50	12.09	4.43	0.02594	0.1728	13.41	0.004335	0.9925	0.1728	0.3747	0.8327	0.5983	0.6740
100	16.70	7.32	0.03551	0.08929	17.79	0.005451	0.9982	0.08929	0.3595	0.8420	0.6239	0.6826
150	21.02	12.85	0.03274	0.04958	23.43	0.002274	0.9962	0.04958	0.2269	0.8496	1.0277	0.8331
200	24.28	16.75	0.03211	0.05952	27.17	0.001841	0.9949	0.05952	0.2005	0.9438	1.1810	0.8719

q_e (exp) and q_e are the experimental and calculated values of q_e, respectively.

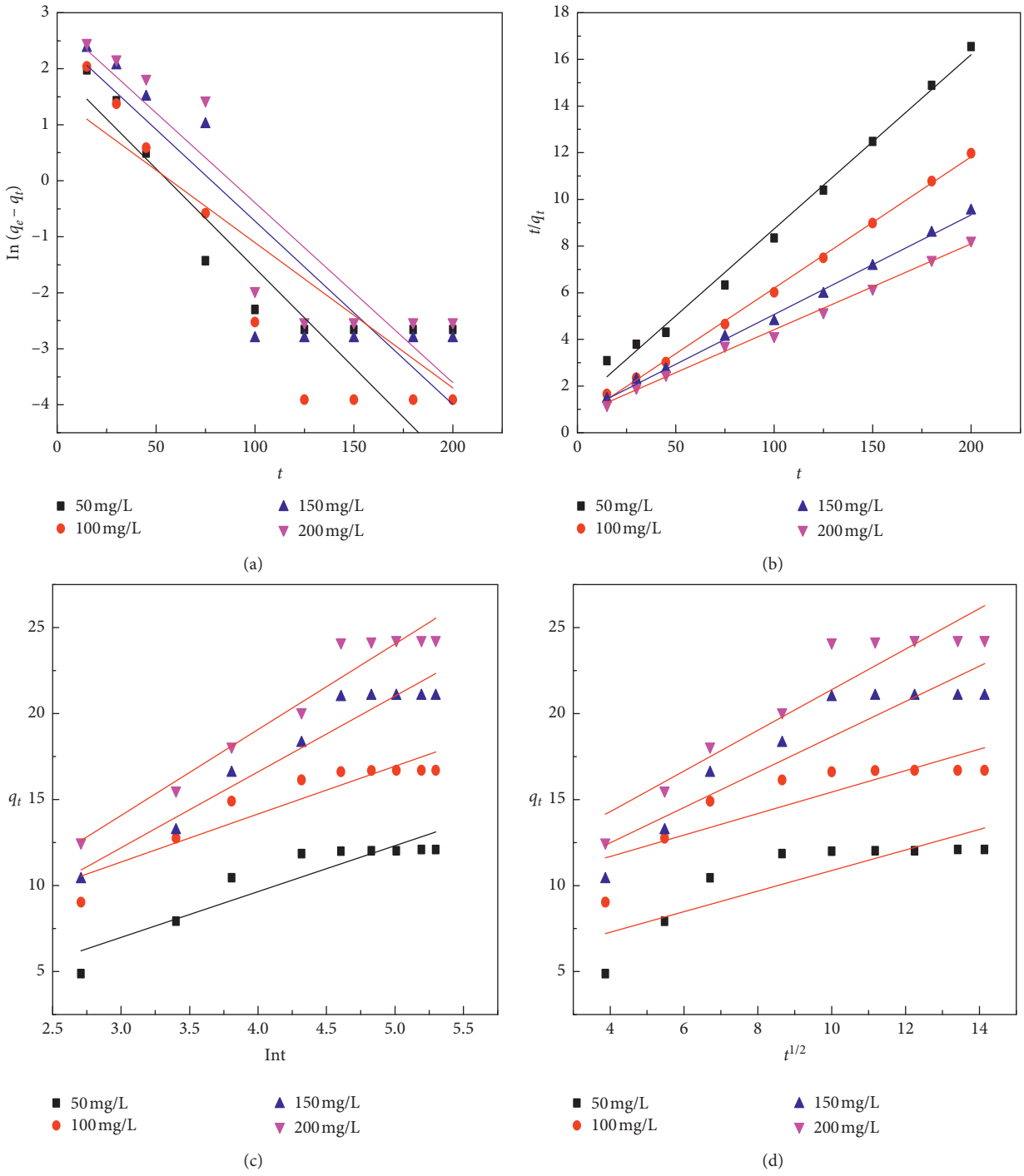

Figure 9: (a) pseudo-first-order, (b) pseudo-second-order, (c) Elovich equation model, and (d) intra-particle diffusion model kinetic plots for ammonia removal by EMRZ at different initial ammonium concentrations (EMRZ dosage = 0.2 g/100 mL; pH value = 6.0; temperature = 25°C).

adsorption process than pseudo-first-order kinetic model under different initial ammonium concentration.

3.8. Adsorption Isotherm. The equilibrium adsorption isotherm is a helpful factor when it comes to the description of the mutually active behavior between solutes and adsorbent, and it is also essential to lay the foundational ground for the design and operation process. The experimental data was matched with the five most widely used isotherm models, Langmuir, Freundlich, Koble–Corrigan, Temkin, and Dubinin–Radushkevich equations, which have been proposed and applied in the literature, to identify the most suitable model [24, 32, 47–49].

3.8.1. Langmuir Isotherm. The Langmuir isotherm model is used to depict the adsorption process occurring at a specific homogeneous location within the EMRZ. The linear form of the Langmuir isotherm model can be calculated by the following formula:

$$\frac{C_e}{q_e} = \frac{1}{q_0 K_L} + \frac{C_e}{q_0}, \tag{3}$$

where K_L is the adsorption equilibrium constant ($L \cdot mg^{-1}$), q_0 is the maximum monolayer adsorption capacity, q_e is the ammonium adsorption capacity at equilibrium time ($mg \cdot g^{-1}$), and C_e is the equilibrium concentration ($mg \cdot L^{-1}$).

As shown in Figure 10, C_e/q_e versus C_e were plotted using the experimental data collected in Figure 6. In addition, Table 2 shows the q_0 and K_L values, which were, respectively, calculated according to the linear plot. The values of q_0 at 25°C, 30°C, and 35°C were obtained as 31.08, 32.05, and 32.88 mg/g, respectively, and were higher than the experimental data (24.14 mg/g at 25°C, 25.28 mg/g at 30°C, and 27.89 mg/g at 35°C). The values of K_L were 0.0205 L/mg at 25°C, 0.02653 L/mg at 30°C, and 0.03354 L/mg at 35°C, which show an increasing trend with temperature increase. It can be inferred that ammonium adsorption is an endothermic process. And the values of correlation coefficients (R^2) were 0.9699, 0.9856, and 0.9886 at 25°C, 30°C, and 35°C, respectively.

Moreover, the basic characteristics of Langmuir isotherms can be expressed by dimensionless separation factors (R_L). And R_L is denoted as follows [25]:

$$R_L = \frac{1}{(1 + K_L C_0)}, \tag{4}$$

where C_0 is the highest initial solute concentration ($mg \cdot L^{-1}$) and K_L is the Langmuir's adsorption constant ($L \cdot mg^{-1}$). The R_L value suggests that the adsorption is unfavorable ($R_L > 1$), linear ($R_L = 1$), favorable ($0 < R_L < 1$), and irreversible ($R_L = 0$). The values of R_L in the present investigation have been found in the range 0.13~0.20 depicting that the adsorption of ammonium at all temperatures used is very favorable.

3.8.2. Freundlich Isotherm. The Freundlich isotherm is an empirical equation used to describe heterogeneous systems. Here is how it is expressed:

$$\ln(q_e) = \frac{1}{n} \ln(C_e) + \ln(K_F), \tag{5}$$

where K_F ($(mg \cdot g^{-1})$ $(L \cdot g^{-1})^n$) and $1/n$ are constants, representing adsorption capacity and adsorption intensity, respectively, and C_e and q_e are of the same nature as those in the Langmuir isotherm model.

Freundlich isothermal plots and constants are presented and listed in Figure 11 and Table 2, respectively. The obtained K_F was in the range of 3.2318~5.4319 and showed an increasing trend with temperature increase, again confirming the endothermic nature of ammonium uptake by EMRZ. The values of $1/n$ were also found in the range of 0.3288~0.3978 at all temperatures used, signifying again that

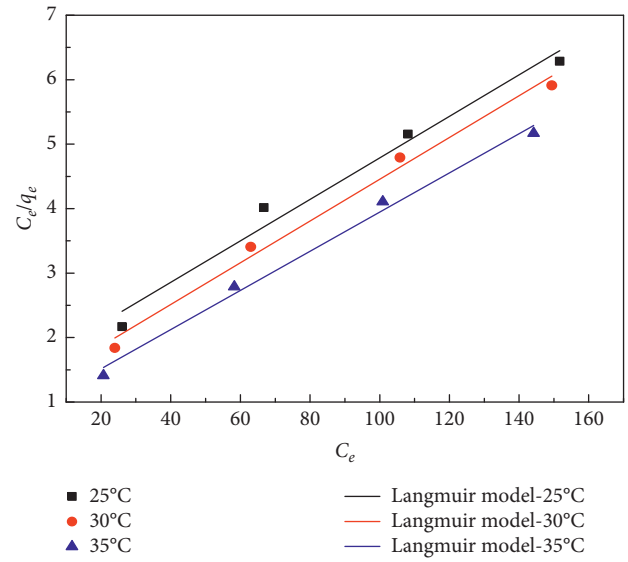

Figure 10: Langmuir isotherm plots for the uptake of ammonium on the EMRZ.

adsorption is favorable. As also seen in Table 2, the correlation coefficients (R^2 between 0.9916 and 0.9996) in the Freundlich isotherm were higher than those in the Langmuir isotherm (R^2 between 0.9699 and 0.9886) for all investigated temperatures. The good adaptability of Freundlich isotherm to experimental data means that heterogeneous surface exists in EMRZ and that the adsorption of ammonia onto EMRZ takes place as a multilayer system [25, 50].

3.8.3. Koble–Corrigan Model. The Koble–Corrigan model is a combination of Langmuir and Freundlich isotherm models. It is expressed in the form below:

$$q_e = \frac{aC_e^n}{1 + bC_e^n}, \tag{6}$$

where a, b, and n are the Koble–Corrigan parameters and C_e and q_e are of the same nature as those in the Langmuir isotherm model.

The experimental and predicted equilibrium data obtained using the Koble–Corrigan model are plotted in Figure 12. Table 2 lists out the obtained Koble–Corrigan parameters, a, b, and n. The correlation coefficients (R^2) for the Koble–Corrigan isotherm model were 0.9945, 0.9990, and 0.9974 at 25°C, 30°C, and 35°C, respectively. In comparison with the Freundlich model, the correlation coefficients (R^2) obtained in Koble–Corrigan model are very similar to those of the Freundlich model. Given the correlation coefficients (R^2) of the Koble–Corrigan and Freundlich models, it was deduced that the main mechanism for the ammonium adsorption process was heterogeneous uptake.

3.8.4. Temkin Isotherm. Temkin isotherm model considers the interaction between adsorbent-adsorbate and the influence of the heat of adsorption of all molecules in the layer.

Table 2: Isotherm constants and regression data of adsorption isotherms of ammonium on EMRZ at different temperatures (EMRZ dosage = 0.2 g/100 mL; contact time = 100 min; pH value = 8.0).

Adsorption isotherm	Temperature (°C)		
	25	30	35
Langmuir isotherm	$K_L = 0.0205$ $q_0 = 31.08$ $R^2 = 0.9699$	$K_L = 0.02653$ $q_0 = 32.05$ $R^2 = 0.9856$	$K_L = 0.03354$ $q_0 = 32.88$ $R^2 = 0.9886$
Freundlich isotherm	$K_F = 3.2318$ $1/n = 0.3978$ $R^2 = 0.9916$	$K_F = 4.1460$ $1/n = 0.3602$ $R^2 = 0.9996$	$K_F = 5.4319$ $1/n = 0.3288$ $R^2 = 0.9988$
Koble–Corrigan isotherm	$a = 3.6079$ $b = -0.2311$ $n = 0.1927$ $R^2 = 0.9945$	$a = 4.3106$ $b = -0.0246$ $n = 0.3261$ $R^2 = 0.9990$	$a = 5.3322$ $b = 0.0161$ $n = 0.3498$ $R^2 = 0.9974$
Temkin isotherm	$A_T = 0.2058$ $B_T = 6.799$ $R^2 = 0.9582$	$A_T = 0.2891$ $B_T = 6.559$ $R^2 = 0.9840$	$A_T = 0.4187$ $B_T = 6.668$ $R^2 = 0.9805$
Dubinin–Radushkevich isotherm	$Q_m = 21.5176$ $K = 6.9309 \times 10^{-5}$ $R^2 = 0.7579$	$Q_m = 22.8728$ $K = 5.4558 \times 10^{-5}$ $R^2 = 0.8200$	$Q_m = 25.2824$ $K = 3.8141 \times 10^{-5}$ $R^2 = 0.8297$

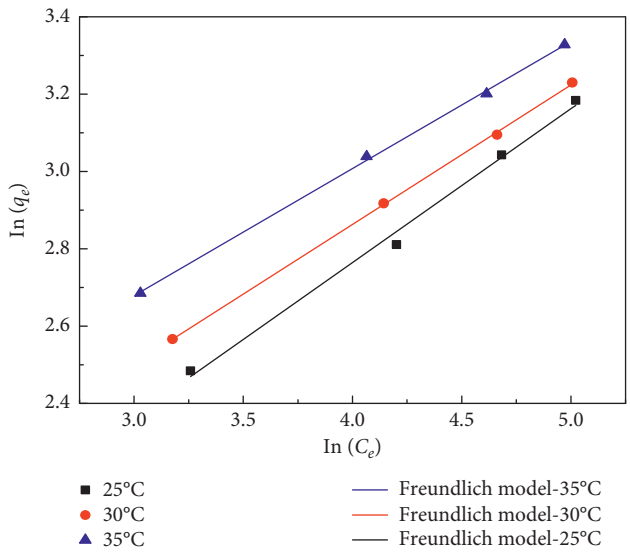

Figure 11: Freundlich isotherm plots for the uptake of ammonium on the EMRZ.

The characteristic of this adsorption is the uniform distribution of binding energies. The Temkin isotherm model can be expressed in the form below:

$$q_e = B_T \ln A_T + B_T \ln C_e, \tag{7}$$

where $B_T = R_T/b$ and b is associated with the heat of adsorption, A_T is the equilibrium binding constant (L/mol), B_T is associated with the heat of adsorption, and C_e and q_e are of the same nature as those in the Langmuir isotherm model.

Figure 13 displays a plot of q_e versus lnC_e at different temperatures. And the Temkin isotherm model parameters and correlation coefficient (R^2) are calculated and listed in Table 2. A_T were 0.2058, 0.2891, and 0.4187 L/mol at 25°C, 30°C, and 35°C, respectively, while B_T were 6.799, 6.559, and 6.668 at those temperatures. And the correlation coefficient (R^2) for Temkin isotherm model was 0.9582 (25°C), 0.9840 (30°C), and 0.9805 (35°C), respectively. As for the correlation coefficient (R^2), the Temkin isotherm model was obviously not so competitive as the Freundlich and Koble–Corrigan isotherm models.

3.8.5. Dubinin–Radushkevich (D–R) Isotherm. The D–R isotherm generally describes the microporous adsorbents adsorption process. And the data were also fitted by D–R isotherm to settle the adsorption type (physical or chemical) [24, 33]. The D–R isotherm model and mean free energy of adsorption (E) can be expressed in the form below:

$$\ln q_e = \ln Q_m - K\varepsilon^2, \tag{8}$$

$$\varepsilon = RT \ln\left(1 + \frac{1}{C_e}\right), \tag{9}$$

$$E = \frac{1}{\sqrt{2K}}, \tag{10}$$

where K is the adsorption energy (mol^2/J^2), Q_m is the theoretical monolayer adsorption capacity (mg/g), and C_e and q_e are of the same nature as those in the Langmuir isotherm model.

Figure 14 and Table 2 show the plots between lnq_e and ε^2 at different temperatures and D–R isotherm model parameters. The Q_m values were found to be 21.5176 mg/g (25°C), 22.8728 mg/g (30°C), and 25.2824 mg/g (35°C), respectively. And values of K were calculated to be 6.9309×10^{-5}, 5.4558×10^{-5}, and 3.8141×10^{-5} at 25°C, 30°C, and 35°C, respectively. Using equation (10), the E value was calculated as 0.08496, 0.09573, and 0.1311 kJ/mol at 25°C, 30°C, and 35°C, respectively. The values of E were found all smaller than 16 kJ/mol, suggesting that the sorption type of ammonium onto EMRZ was physical uptake process. On the other hand, the obtained correlation coefficient (R^2) at 25°C,

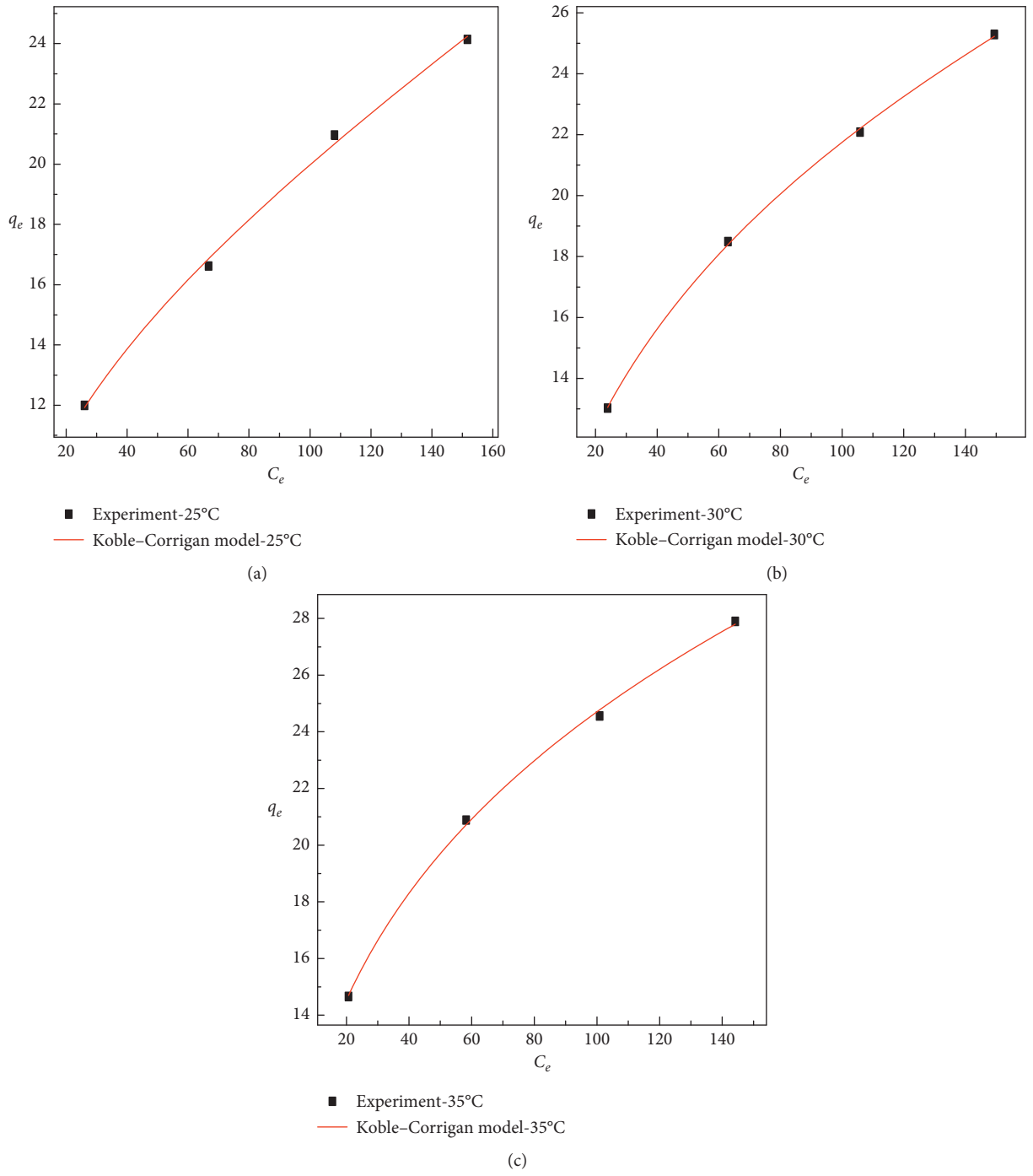

Figure 12: Koble–Corrigan isotherm plots for the uptake of ammonium on the EMRZ.

30°C, and 35°C was 0.7579, 0.8200, and 0.8297, respectively, which are considerably smaller than those obtained from the other isotherm models as displayed in Table 2. Namely, the D–R model is not suitable for describing the experimental equilibrium data.

3.8.6. Summary of the Adsorption Isotherm Studies. To sum up, the above analyses were sufficient in proving that the experimental data are best fitted by the Freundlich and Koble–Corrigan model due to the much higher R^2 (see Table 2). These results are consistent with those reported by other researchers [24, 32, 51].

Table 3 compares ammonium uptake capacities among various zeolites. For the reason that the tests were carried out under different experimental conditions, the comparison between ammonium uptake capacities of EMRZ in this study and those of previously tested zeolites is not a practical one. However, as shown in Table 3, the EMRZ analyzed in this work is with a greater capacity for ammonia adsorption

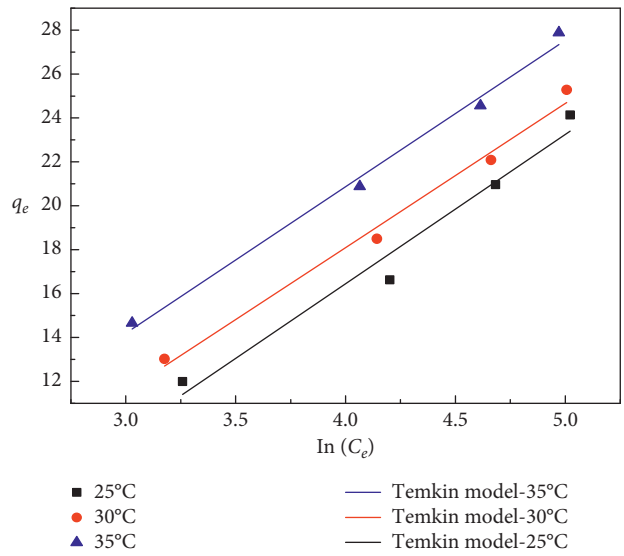

Figure 13: Temkin isotherm plots for the uptake of ammonium on the EMRZ.

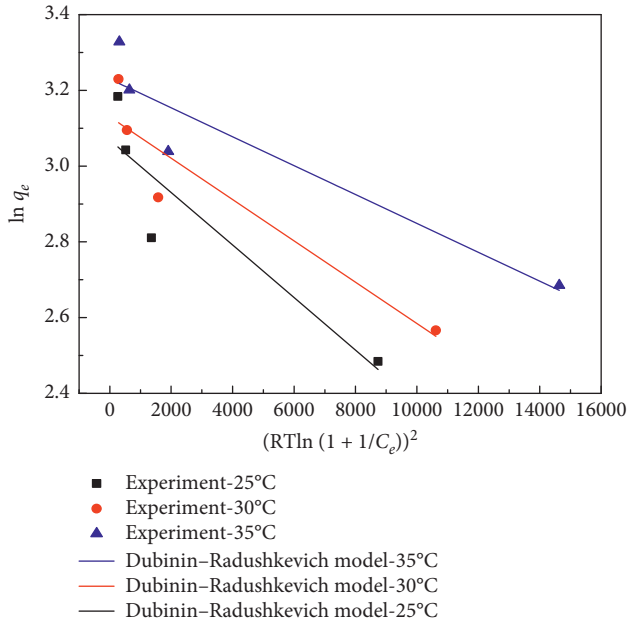

Figure 14: D–R isotherm plots for the uptake of ammonium on the EMRZ.

and it shows huge potential in serving as an effective adsorbent for ammonia. Moreover, utilizing EMR to prepare EMRZ not only contributes to reduction of waste generation but also boosts cost efficiency. Thus, the obtained EMRZ, as an adsorbent for ammonium removal, is both readily accessible and highly efficient.

3.9. Adsorption Thermodynamics. Thermodynamic parameters, like enthalpy (ΔH°), Gibbs energy (ΔG°), and entropy (ΔS°), for the adsorption of ammonium on EMRZ were calculated from Langmuir constant at different temperatures (25°C, 30°C, and 35°C) using the following equations:

Table 3: Comparison of maximum adsorption capacity of ammonium on various zeolites.

Adsorbent	Maximum adsorption capacity (mg/g)	Reference
EMRZ	31.08~32.88	This work
Natural Chinese zeolite	5.87~6.02	[52]
Natural Chinese clinoptilolite	10.53	[53]
Natural Iranian zeolite	8.51–10.39	[42]
Natural Iranian zeolite	43.47	[54]
Pretreated natural zeolites	32.73	[55]
NaCl-modified zeolite	14.26	[48]
NaOH-activated zeolite	21.2	[46]
Natural Turkish zeolite	5.76–7.36	[56]
Rice husk ash-synthesized zeolite	42.37	[25]
Fly ash derived zeolite	18.19	[57]
Fly ash derived zeolite	3.94	[58]

$$\ln K_L = -\frac{\Delta^{H^\circ}}{RT} + \frac{\Delta^{S^\circ}}{R},$$
$$\Delta^{G^\circ} = \Delta^{H^\circ} - T\Delta^{S^\circ}. \quad (11)$$

The values of ΔH°, ΔG°, and ΔS° parameters are summarized in Table 4. The free energy changes (ΔG) obtained were −14.03, −14.90, and −15.77 kJ mol^{-1} at 25°C, 30°C, and 35°C, respectively. The negative values of ΔG suggest ammonium uptake by EMRZ is spontaneous. And the greater the negative value of ΔG goes, the more energetically favorable the adsorption becomes. The enthalpy (ΔH) was +37.66 kJ mol^{-1}; therefore, ammonium uptake by EMRZ is an endothermic process. This confirms the adsorption isotherm studies in Section 3.8. Also, the positive value of entropy ($\Delta S = +173.38$ J·mol^{-1}·K^{-1}) indicates that the randomness of the solid-solution interface increases during the adsorption of the ammonium to the EMRZ.

3.10. Reuse Performance of EMRZ. In order to evaluate the reuse performance of EMRZ on the ammonium uptake performance, the ammonium uptake capacity of regenerated EMRZ was investigated and compared with fresh EMRZ under different pH values and cycle times [59]. The ammonium uptake capacity by the regenerated EMRZ with different pH values and cycle times is shown in Figure 15. As seen in Figure 15(a), the maximum uptake capacity of the first regenerated EMRZ also occurred at pH 8.0, and a small fall of 0.69 mg/g on the ammonium uptake capacity was observed comparing the regenerated and fresh EMRZ. On the other hand, it is obvious that the ammonium uptake capacity decreases moderately with the increase of cycle times from 18.20 mg/g for the fresh EMRZ to 14.43 mg/g for the fifth cycle (see Figure 15(b)). Therefore, these results still show that there was no clear deterioration observed for the regenerated EMRZ. And this finding was consistent with the report of Li et al. [60], Huang et al. [61], and Alshameri et al. [35]. Moreover, the efficient utilization of EMR as

Table 4: Thermodynamic parameters for the adsorption of ammonium onto EMRZ.

Adsorbent	ΔG (kJ·mol^{-1})			ΔH (kJ·mol^{-1})	ΔS (J·mol^{-1}·K^{-1})
	25°C	30°C	35°C		
EMRZ	−14.03	−14.90	−15.77	+37.66	+173.38

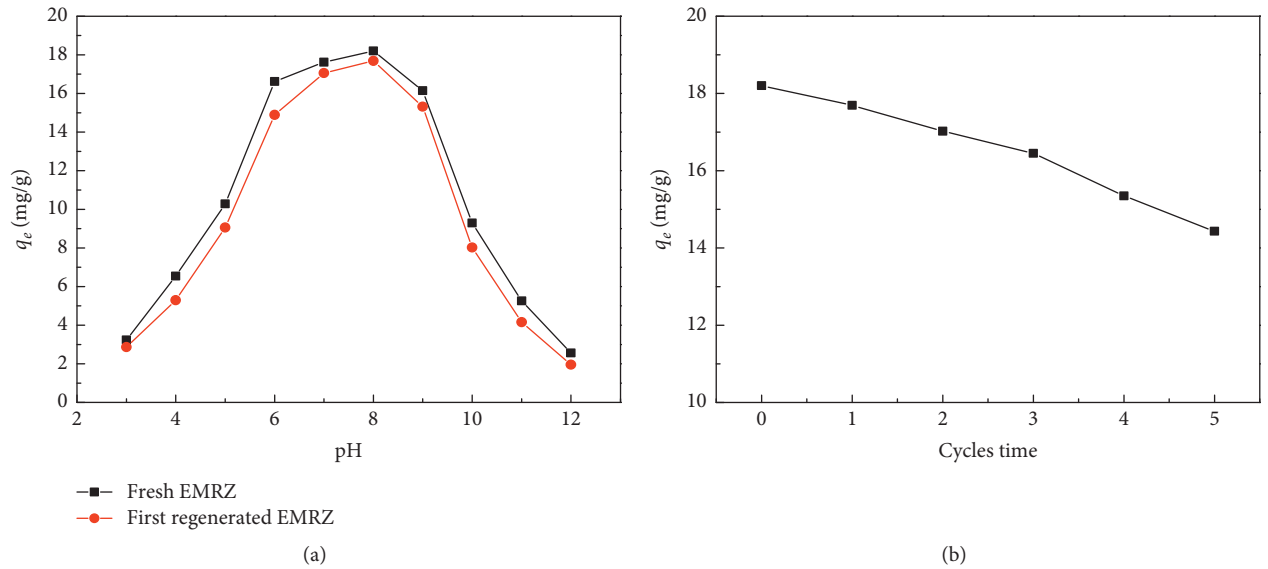

Figure 15: Comparison of ammonium uptake capacity by fresh and regenerated EMRZ. (a) EMRZ dosage = 0.2 g/100 mL; initial ammonium concentration = 100 mg/L; temperature = 25°C; contact time = 100 min. (b) EMRZ dosage = 0.2 g/100 mL; initial ammonium concentration = 100 mg/L; temperature = 25°C; contact time = 100 min; pH value = 8.0.

ingredients of EMRZ may be advantageous in reduction of not only waste generation but also manufacturing costs.

4. Conclusions

EMR can be converted into EMR-based zeolite (EMRZ) via a fusion method, as confirmed by XRD and SEM analyses. And the major crystalline component of the synthesized EMRZ was detected as zeolite A. The performance for ammonium uptake of EMRZ is dependent upon the contact time, EMRZ dosage, initial ammonium concentration, and pH value. The most favorable pH for ammonium uptake by the EMRZ was obtained at 8.0, and the equilibrium adsorption was rapidly attained within 100 min. The presence of both competitive cations and anions also affected ammonium uptake. The orders $Na^+ > K^+ > Ca^{2+} > Mg^{2+}$ for cations and $CO_3^{2-} > Cl^- > SO_4^{2-} > PO_4^{3-}$ for anions were observed. The adsorption kinetics is best approximated by the pseudo-second-order model. The Freundlich and Koble–Corrigan adsorption isotherm model are best fitted by the equilibrium data, suggesting that heterogeneous uptake was the principal mechanism adopted in the process of ammonium adsorption. This study identified thermodynamic parameters as well. The negative values of ΔG indicate that ammonium uptake onto EMRZ is spontaneous process. The enthalpy (ΔH) and the entropy changes (ΔS) were both positive meaning endothermic adsorption process and increasing the randomness of the solid-solution interface during the adsorption of the ammonium to the EMRZ. The reuse of EMRZ could achieve a good ammonium uptake capacity, and there was no clear deterioration observed for the regenerated EMRZ. This study demonstrates that the EMRZ can be successfully used as a suitable and efficient adsorbent for removing ammonium from aqueous solutions.

Data Availability

The data used to support the findings of this study are available from the corresponding author upon request.

Conflicts of Interest

The authors declare that they have no conflicts of interest.

Acknowledgments

The authors are grateful for the project funded by China Postdoctoral Science Foundation (No. 2017M611799) and Jiangsu Provincial Basic Research Program (Natural Science Foundation)-Youth Foundation Project (No. BK20190690) and Hunan Provincial Science and Technology Plan Project, China (No. 2016TP1007), by offering the research fund.

References

[1] H. Paerl, "Doing battle with the green monster of Taihu lake," *Science*, vol. 317, p. 1166, 2007.

[2] M. Yang, J. Yu, Z. Li, Z. Guo, M. Burch, and T.-F. Lin, "Taihu lake not to blame for Wuxi's woes," *Science*, vol. 319, no. 5860, p. 158a, 2008.

[3] D. J. Randall and T. K. N. Tsui, "Ammonia toxicity in fish," *Marine Pollution Bulletin*, vol. 45, no. 1–12, pp. 17–23, 2002.

[4] M. Iqbal, "Vicia faba bioassay for environmental toxicity monitoring: a review," *Chemosphere*, vol. 144, pp. 785–802, 2016.

[5] M. Abbas, M. Adil, S. Ehtisham-Ul-Haque et al., "Vibrio fischeri bioluminescence inhibition assay for ecotoxicity assessment: a review," *Science of the Total Environment*, vol. 626, pp. 1295–1309, 2018.

[6] M. Iqbal, M. Abbas, J. Nisar et al., "Bioassays based on higher plants as excellent dosimeters for ecotoxicity monitoring: a review," *Chemistry International*, vol. 5, no. 1, pp. 1–80, 2019.

[7] M. Sprynskyy, M. Lebedynets, A. P. Terzyk, P. Kowalczyk, J. Namieśnik, and B. Buszewski, "Ammonium sorption from aqueous solutions by the natural zeolite Transcarpathian clinoptilolite studied under dynamic conditions," *Journal of Colloid and Interface Science*, vol. 284, no. 2, pp. 408–415, 2005.

[8] M. L. Nguyen and C. C. Tanner, "Ammonium removal from wastewaters using natural New Zealand zeolites," *New Zealand Journal of Agricultural Research*, vol. 41, no. 3, pp. 427–446, 1998.

[9] M. Lebedynets, M. Sprynskyy, I. Sakhnyuk et al., "Adsorption of ammonium ions onto a natural zeolite: transcarpathian clinoptilolite," *Adsorption Science & Technology*, vol. 22, no. 9, pp. 731–741, 2004.

[10] E. Marañón, M. Ulmanu, Y. Fernández, I. Anger, and L. Castrillón, "Removal of ammonium from aqueous solutions with volcanic tuff," *Journal of Hazardous Materials*, vol. 137, no. 3, pp. 1402–1409, 2006.

[11] B. Makgabutlane, L. N. Nthunya, N. Musyoka, B. S. Dladla, E. N. Nxumalo, and S. D. Mhlanga, "Microwave-assisted synthesis of coal fly ash-based zeolites for removal of ammonium from urine," *RSC Advances*, vol. 10, no. 4, p. 2416, 2020.

[12] L. Gao, C. Y. Zhang, Y. Sun et al., "Effect and mechanism of modification treatment on ammonium and phosphate removal by ferric-modified zeolite," *Environmental Technology*, vol. 40, no. 13–16, pp. 1959–1968, 2019.

[13] C. Li, Y. Yu, Q. Li, H. Zhong, and S. Wang, "Kinetics and equilibrium studies of phosphate removal from aqueous solution by calcium silicate hydrate synthesized from electrolytic manganese residue," *Adsorption Science & Technology*, vol. 37, no. 7-8, pp. 547–565, 2019.

[14] C. X. Li, H. Zhong, S. Wang et al., "Leaching behavior and risk assessment of heavy metals in a landfill of electrolytic manganese residue in western Hunan, China," *Human and Ecological Risk Assessment*, vol. 20, no. 5-6, pp. 1249–1263, 2014.

[15] C.-x. Li, H. Zhong, S. Wang, J.-r. Xue, F.-f. Wu, and Z.-y. Zhang, "Preparation of MnO2 and calcium silicate hydrate from electrolytic manganese residue and evaluation of adsorption properties," *Journal of Central South University*, vol. 22, no. 7, pp. 2493–2502, 2015.

[16] A. Habib, H. N. Bhatti, and M. Iqbal, "Metallurgical processing strategies for metals recovery from industrial slags," *Ztschrift für Physikalische Chemie*, vol. 234, pp. 201–231, 2020.

[17] M. Rahmat, A. Rehman, S. Rahmat et al., "Laser ablation assisted preparation of MnO2 nanocolloids from waste battery cell powder: evaluation of physico-chemical, electrical and biological properties," *Journal of Molecular Structure*, vol. 1191, pp. 284–290, 2019.

[18] M. Rahmat, A. Rehman, S. Rahmat et al., "Highly efficient removal of crystal violet dye from water by MnO2 based nanofibrous mesh/photocatalytic process," *Journal of Materials Research and Technology*, vol. 8, no. 6, pp. 5149–5159, 2019.

[19] Z. Milan, E. Sánchez, P. Weiland et al., "Ammonia removal from anaerobically treated piggery manure by ion exchange in columns packed with homoionic zeolite," *Chemical Engineering Journal*, vol. 66, no. 1, pp. 65–71, 1997.

[20] N. A. Booker, E. L. Cooney, and A. J. Priestley, "Ammonia removal from sewage using natural Australian zeolite," *Water Science and Technology*, vol. 34, no. 9, pp. 17–24, 1996.

[21] L. R. Weatherley and N. D. Miladinovic, "Comparison of the ion exchange uptake of ammonium ion onto New Zealand clinoptilolite and mordenite," *Water Research*, vol. 38, no. 20, pp. 4305–4312, 2004.

[22] C. Li, H. Zhong, S. Wang, J. Xue, and Z. Zhang, "Removal of basic dye (methylene blue) from aqueous solution using zeolite synthesized from electrolytic manganese residue," *Journal of Industrial and Engineering Chemistry*, vol. 23, pp. 344–352, 2015.

[23] M. Y. Li, X. Q. Zhu, F. H. Zhu et al., "Application of modified zeolite for ammonium removal from drinking water," *Desalination*, vol. 271, no. 1–3, pp. 295–300, 2011.

[24] M. Zhang, H. Zhang, D. Xu et al., "Removal of ammonium from aqueous solutions using zeolite synthesized from fly ash by a fusion method," *Desalination*, vol. 271, no. 1–3, pp. 111–121, 2011.

[25] A. M. Yusof, L. K. Keat, Z. Ibrahim et al., "Kinetic and equilibrium studies of the removal of ammonium ions from aqueous solution by rice husk ash-synthesized zeolite Y and powdered and granulated forms of mordenite," *Journal of Hazardous Materials*, vol. 174, no. 1–3, pp. 380–385, 2010.

[26] S. M. Ahari, R. J. Yangejeh, A. H. Mahvi et al., "A new method for the removal of ammonium from drinking water using hybrid method of modified zeolites/catalytic ozonation," *Desalination and Water Treatment*, vol. 170, pp. 148–157, 2019.

[27] H. Tang, X. Xu, B. Wang, C. Lv, and D. Shi, "Removal of ammonium from swine wastewater using synthesized zeolite from fly ash," *Sustainability*, vol. 12, no. 8, p. 3423, 2020.

[28] H. M. Huang, X. M. Xiao, B. Yan et al., "Ammonium removal from aqueous solutions by using natural Chinese (Chende) zeolite as adsorbent," *Journal of Hazardous Materials*, vol. 175, no. 1–3, pp. 247–252, 2010.

[29] Q. Du, S. Liu, Z. Cao, and Y. Wang, "Ammonia removal from aqueous solution using natural Chinese clinoptilolite," *Separation and Purification Technology*, vol. 44, no. 3, pp. 229–234, 2005.

[30] H. N. Bhatti, J. Hayat, M. Iqbal, S. Noreen, and S. Nawaz, "Biocomposite application for the phosphate ions removal in aqueous medium," *Journal of Materials Research and Technology*, vol. 7, no. 3, pp. 300–307, 2018.

[31] A. M. Awwad, M. W. Amer, and M. M. Al-aqarbeh, "TiO_2-kaolinite nanocomposite prepared from the Jordanian Kaolin clay: adsorption and thermodynamic of Pb (II) and Cd (II) ions in aqueous solution," *Chemistry International*, vol. 6, no. 4, pp. 168–178, 2020.

[32] N. Widiastuti, H. W. Wu, H. M. Ang et al., "Removal of ammonium from greywater using natural zeolite," *Desalination*, vol. 277, no. 1–3, pp. 15–23, 2011.

[33] K. Saltalı, A. Sarı, and M. Aydın, "Removal of ammonium ion from aqueous solution by natural Turkish (Yıldızeli) zeolite for environmental quality," *Journal of Hazardous Materials*, vol. 141, no. 1, pp. 258–263, 2007.

[34] D. Karadag, Y. Koc, M. Turan, and B. Armagan, "Removal of ammonium ion from aqueous solution using natural Turkish clinoptilolite," *Journal of Hazardous Materials*, vol. 136, no. 3, pp. 604–609, 2006.

[35] A. Alshameri, C. Yan, Y. Al-Ani et al., "An investigation into the adsorption removal of ammonium by salt activated Chinese (Hulaodu) natural zeolite: kinetics, isotherms, and thermodynamics," *Journal of the Taiwan Institute of Chemical Engineers*, vol. 45, no. 2, pp. 554–564, 2014.

[36] Z. Wu, J. Xie, H. Liu et al., "Preparation, characterization, and performance of 4A zeolite based on opal waste rock for removal of ammonium ion," *Adsorption Science and Technology*, vol. 36, pp. 1–16, 2018.

[37] L. T. Nanganoa, G. T. Merlain, J. N. Ndi et al., "Removal of ammonium ions from aqueous solution using hydroxy-sodalite zeolite," *Asian Journal of Green Chemistry*, vol. 3, pp. 169–186, 2019.

[38] D. T. N. Wijesinghe, K. B. Dassanayake, P. J. Scales, S. G. Sommer, and D. Chen, "Effect of Australian zeolite on methane production and ammonium removal during anaerobic digestion of swine manure," *Journal of Environmental Chemical Engineering*, vol. 6, no. 1, pp. 1233–1241, 2018.

[39] L. Lei, X. Li, and X. Zhang, "Ammonium removal from aqueous solutions using microwave-treated natural Chinese zeolite," *Separation and Purification Technology*, vol. 58, no. 3, pp. 359–366, 2008.

[40] Y. F. Wang, F. Lin, and W. Q. Pang, "Ammonium exchange in aqueous solution using Chinese natural clinoptilolite and modified zeolite," *Journal of Hazardous Materials*, vol. 142, no. 1-2, pp. 160–164, 2007.

[41] D. Karadag, S. Tok, E. Akgul et al., "Ammonium removal from sanitary landfill leachate using natural Goerdes clinoptilolite," *Journal of Hazardous Materials*, vol. 153, no. 1-2, pp. 60–66, 2008.

[42] F. Mazloomi and M. Jalali, "Ammonium removal from aqueous solutions by natural Iranian zeolite in the presence of organic acids, cations and anions," *Journal of Environmental Chemical Engineering*, vol. 4, no. 1, pp. 240–249, 2016.

[43] M. M. Al-a'qarbeh, M. W. Shammout, and A. M. Awwad, "Nano platelets kaolinite for the adsorption of toxic metal ions in the environment," *Chemistry International*, vol. 6, no. 2, pp. 49–55, 2020.

[44] E. C. Jennifer and O. P. Ifedi, "Modification of natural bentonite clay using cetyl trimetyl-ammonium bromide and its adsorption capability on some petrochemical wastes," *Chemistry International*, vol. 5, no. 4, pp. 269–273, 2019.

[45] Y. Cheng, T. Huang, X. Shi, G. Wen, and Y. Sun, "Removal of ammonium ion from water by Na-rich birnessite: performance and mechanisms," *Journal of Environmental Sciences*, vol. 57, no. 7, pp. 402–410, 2017.

[46] Y. He, H. Lin, Y. Dong, Q. Liu, and L. Wang, "Simultaneous removal of ammonium and phosphate by alkaline-activated and lanthanum-impregnated zeolite," *Chemosphere*, vol. 164, pp. 387–395, 2016.

[47] J. S. Cyrus and G. B. Reddy, "Sorption and desorption of ammonium by zeolite: batch and column studies," *Journal of Environmental Science and Health, Part A*, vol. 46, no. 4, pp. 408–414, 2011.

[48] L. Lin, Z. Lei, L. Wang et al., "Adsorption mechanisms of high-levels of ammonium onto natural and NaCl-modified zeolites," *Separation and Purification Technology*, vol. 103, no. 15, pp. 15–20, 2013.

[49] Y. Zhao, Y. C. Niu, X. Hu et al., "Removal of ammonium ions from aqueous solutions using zeolite synthesized from red mud," *Desalination & Water Treatment*, vol. 57, pp. 1–12, 2015.

[50] G. Moussavi, S. Talebi, M. Farrokhi, and R. M. Sabouti, "The investigation of mechanism, kinetic and isotherm of ammonia and humic acid co-adsorption onto natural zeolite," *Chemical Engineering Journal*, vol. 171, no. 3, pp. 1159–1169, 2011.

[51] M. Sarioglu, "Removal of ammonium from municipal wastewater using natural Turkish (Dogantepe) zeolite," *Separation and Purification Technology*, vol. 41, no. 1, pp. 1–11, 2005.

[52] Z. H. Ye, J. W. Wang, L. Y. Sun et al., "Removal of ammonium from municipal landfill leachate using natural zeolites," *Environmental Technology*, vol. 36, no. 21–24, pp. 2919–2923, 2015.

[53] Y. Zhang and E. Bi, "Effect of dissolved organic matter on ammonium sorption kinetics and equilibrium to Chinese clinoptilolite," *Environmental Technology*, vol. 33, no. 19–21, pp. 2395–2403, 2012.

[54] A. Khosravi, M. Esmhosseini, and S. Khezri, "Removal of ammonium ion from aqueous solutions using natural zeolite: kinetic, equilibrium and thermodynamic studies," *Research on Chemical Intermediates*, vol. 40, no. 8, pp. 2905–2917, 2014.

[55] C. Glass and R. C. Wah, "Enhancement of ammonium adsorption capacity with pretreated natural zeolites," *Habitation*, vol. 12, no. 1, pp. 97–102, 2009.

[56] D. Karadag, Y. Koc, M. Turan et al., "A comparative study of linear and non-linear regression analysis for ammonium exchange by clinoptilolite zeolite," *Journal of Hazardous Materials*, vol. 144, no. 1-2, pp. 432–437, 2007.

[57] M. L. Zhang, H. Y. Zhang, D. Xu et al., "Ammonium removal from aqueous solution by zeolites synthesized from low-calcium and high-calcium fly ashes," *Desalination*, vol. 277, no. 1–3, pp. 46–53, 2011.

[58] Y. Wang, J. Y. Chen, X. M. Li et al., "Simultaneous removal of ammonium and phosphate in waste water by La-modified synthetic zeolite from coal fly ash," *China Environmental Science*, vol. 31, no. 7, pp. 1152–1158, 2011.

[59] K. Wu, Y. Li, T. Liu et al., "Evaluation of the adsorption of ammonium-nitrogen and phosphate on a granular composite adsorbent derived from zeolite," *Environmental Science and Pollution Research*, vol. 26, no. 17, pp. 17632–17643, 2019.

[60] M. Li, C. Feng, Z. Zhang, X. Lei, N. Chen, and N. Sugiura, "Simultaneous regeneration of zeolites and removal of ammonia using an electrochemical method," *Microporous and Mesoporous Materials*, vol. 127, no. 3, pp. 161–166, 2010.

[61] H. Huang, L. Yang, Q. Xue, J. Liu, L. Hou, and L. Ding, "Removal of ammonium from swine wastewater by zeolite combined with chlorination for regeneration," *Journal of Environmental Management*, vol. 160, pp. 333–341, 2015.